

Sediment infill of the Middle Triassic half-graben below Mt. Vernar in the Julian Alps, Slovenia

Luka Gale^{1,2(*)}, Katarina Kadivec^{1,3}, Marko Vrabc¹ and Bogomir Celarc^{2†}

¹ University of Ljubljana, Department of Geology, Aškerčeva 12, 1000 Ljubljana, Slovenia;

(*corresponding author ORCID No. 0000-0002-2524-0073 luka.gale@ntf.uni-lj.si; marko.vrabc@ntf.uni-lj.si)

² Geological Survey of Slovenia, Dimičeva 14, 1000 Ljubljana, Slovenia; (luka.gale@geo-zs.si)

³ IRGO Consulting d.o.o., Slovenčeva 93, 1000 Ljubljana, Slovenia; (katarina.kadivec@irgo.si)

doi: 10.4154/gc.2023.03



Abstract

A sediment infill of a small, late Anisian–earliest Ladinian half-graben, sealed by massive limestone of the Schlern Formation is exposed on the northeastern slopes of Mt. Vernar in the eastern Julian Alps, Slovenia. The pre-rift base of the succession is formed by a chaotic mixture of massive limestone and limestone breccia of the Anisian platform. Sedimentation in the half-graben started with a 20 m thick thinly bedded pink nodular limestone which is informally named here as the Vernar member. It consists of microbial carbonate and was probably deposited within the photic zone. The Vernar member is overlain by poorly sorted polymict breccias of the Uggowitz Breccia Formation which reaches a thickness of at least 150 m, but pinches out rapidly towards the SE graben margin, reflecting the highly asymmetric basin geometry. Individual beds of breccia represent successive debris flow deposits. The Uggowitz Breccia Formation is followed by a few metres of sandstone and sandy limestone of the Buchenstein Formation. The limestone contains abundant grains of shallow marine origin and terrestrial plant fragments. The overlying post-rift Schlern Formation consists of crudely bedded and massive limestone, covering the graben. The consistent NE-SW strike of the graben-bounding faults and of the small-scale conjugate normal faults observed in the Uggowitz Breccia Formation suggests that the half-graben originated from NW-SE directed extension.

Article history:

Manuscript received October 08, 2022

Revised manuscript accepted December 29, 2022

Available online February 23, 2023

Keywords: Southern Alps, Middle Triassic, half-graben, Uggowitz Breccia, debris-flow deposits

1. INTRODUCTION

During the early and middle Anisian, the western margin of the Palaeotethys Ocean of the present Dinaric-Carpathian-Alpine region was characterised by relatively uniform sedimentation (HAAS et al., 1995; KOVÁCS et al., 2011). Sea level changes were strongly expressed in the more landward-located areas, such as in the present-day central and western Southern Alps (GIANOLLA et al., 1998; MIETTO et al., 2020), whereas they had limited or no effect in the more oceanward positioned platform of the present-day eastern Southern Alps (BUSER, 1989). The relatively widespread and uniform sedimentary conditions were terminated during the late Anisian due to the more vigorous transtensional tectonics, and a more differentiated topography was established (BUSER, 1989; HAAS & BUDAI, 1999; BUDAI & VÖRÖS, 2006; BALINI ET AL., 2006; BERRA & CARMINATI, 2010; STEFANI et al., 2010; VELLEDDITS et al., 2011; GAWLICK et al., 2012; MIETTO et al., 2020; SMIRČIĆ et al., 2020). Extension of the upper crust is evidenced in the area of the present-day Julian, Carnic, and Kamnik-Savinja Alps, as well as in the Karavanke Mts. in the formation of a number of small-scale half-grabens filled with breccia and conglomerate of the so-called Uggowitz (Ugovizza) Breccia Formation (FARABEGOLI et al., 1985; VENTURINI, 1990; KOZUR et al., 1994; KRAINER & LUTZ, 1995; CELARC et al., 2013). The Uggowitz Breccia Formation was deposited in a variety of settings and the stratigraphic successions vary. In the Carnic Alps, it forms the basal part of a transgressive sequence and is interpreted as a fluvial or deltaic depositional unit (e.g., FARABEGOLI & LEVANTI, 1982; FARABEGOLI et al., 1985; VENTURINI, 1990, 2006). In contrast, in the Karavanke Mts., in the Julian Alps, and in the Kamnik-

Savinja Alps, the Uggowitz Breccia Formation is under- and overlain by deeper-marine sediments (KOZUR et al., 1994; CELARC et al., 2013). Contemporary regional volcanism added to the lithological diversity resulting from the interplay between tectonics, sea level changes and carbonate production (BUSER, 1989; BOSELLINI et al., 2003; MIETTO et al., 2020).

CELARC et al. (2013) described the Uggowitz Breccia Formation occurrences in the Kamnik-Savinja Alps, but other exposures in the eastern Southern Alps remain undescribed or are only briefly mentioned. The aim of this research is to present a detailed sedimentological analysis of the Uggowitz Breccia Formation underlying the Schlern Formation of Mt. Vernar in the Julian Alps (Slovenia). The succession was briefly mentioned by JURKOVŠEK (1987) and RAMOVŠ (2000) but was never investigated in detail. Here, we aim to interpret the mechanism of deposition and the depositional environment for the described units, and to offer an interpretation of the basin evolution.

2. GEOLOGICAL SETTING

Mt. Vernar (lat. 46°21'36.25", long. 13°51'46.62") is a 2225 m a.s.l. high mountain in the Julian Alps, NW Slovenia, a part of the eastern Southern Alps (Fig. 1A). The structure of the Julian Alps is largely governed by the two Alpine thrust systems: the Maas-trichtian to Eocene SW- to W-vergent Dinaric system, and the late Oligocene–early Miocene S- to SE-vergent South Alpine thrusts. Neotectonic NNW-directed shortening starting in the Late Miocene-Pliocene and produced NW-SE-striking dextral and NE-SW striking sinistral faults which displace the thrusts (Fig. 1B) (POLI & ZANFERARRI, 1995; CASTELLARIN & CANTELLI, 2000; PLACER, 2008; CAPUTO et al., 2010,

GORIČAN et al., 2018, 2022). Mt. Vernar sits in the Dinaric Zlatna Klippe, which occupies the highest structural position and lies over the South Alpine Krn Nappe (Fig. 1B) (JURKOVŠEK, 1986, 1987; GORIČAN et al., 2012, 2018).

Previous research in the Julian Alps and the Kamnik-Savinja Alps (CELARC et al., 2013) showed that the carbonate platforms of the eastern South Alpine domain were drowned during the late Anisian. Locally formed half-grabens were filled with pelagic red nodular limestone (the Loibl Formation), pyroclastics, and rhyolites or carbonate breccia (the Uggowitz Breccia Formation), and finally by thin-bedded limestone, grainstone, and subordinate marl (the Buchenstein Formation). A carbonate platform (the Schlern Formation) then prograded over the wider area and sealed the half-grabens (CELARC et al., 2013).

3. MATERIAL AND METHODS

The area of Mt. Vernar and its surroundings was mapped at a 1:5.000 scale. Since a large part of this area is inaccessible due to rugged alpine terrain, the NE face of Mt. Vernar was also surveyed with an unmanned aerial vehicle (UAV) DJI Phantom 4 Pro and then a 3D model of the exposure was created using Structure-from-Motion photogrammetry in Metashape Pro modelling software to get additional insight into the structure and stratigraphy of the subvertical sections of the mountain. The stratigraphic succession of the NE slope of Mt. Vernar was logged and sampled in four sections. Fifty-eight samples were taken from in-situ beds. An additional 29 samples were taken from scree deposits. Of these, 10 samples belong to the Uggowitz Breccia Formation, and 19 are derived from the overlying platform (Schlern Formation). Samples from the scree were considered only when their origin was undisputed and only as additional samples. Biostratigraphic interpretations are not based on these samples. Thin sections of 28 × 47 mm and 75 × 49 mm sizes were made and analysed with a polarizing microscope. Carbonates were classified according to DUNHAM (1962), and EMBRY and KLOVAN (1971). As suggested by WRIGHT (1992), we use the term calcimudstone as a

texture of carbonate rocks as opposed to mudstone used for siliciclastic rocks. The terminology employed for microbial carbonate follows RIDING (2000).

4. RESULTS

4.1. General stratigraphy and structure

The logged succession begins with thin-bedded, often nodular pinkish limestone some 20 m thick, which only outcrops in the SE part of the exposure (Figs. 2, 3). It is informally named here as the Vernar member. To the SE, the Vernar member laterally passes into a chaotic mixture of massive grey limestone and monomictic breccias, which probably belong to the upper Anisian Contrin Formation. We interpret this contact as a NW-dipping low-angle normal fault zone, separating the Vernar member from the underlying Contrin Formation (Fig. 3A). The pinkish limestone of the Vernar member is cut by Neptunian dykes filled with polymictic breccia, identical to the breccias of the overlying Uggowitz Breccia Formation. The topmost layers of the Vernar member overlying the normal fault zone are not affected by faulting, suggesting that the fault was active during sedimentation and that its activity terminated before the end of deposition of the Vernar member.

The Vernar member is overlain by a few beds of poorly sorted polymict breccias of the Uggowitz Breccia Formation (Figs. 2, 3A). Towards the SE, these beds pinch out entirely. North-westward, less than 20 m from the Vernar member outcrop, the thickness of the Uggowitz Breccia Formation rapidly increases to 35 m (section 2 in Fig. 2), and then to more than 150 m in a large outcrop about 150 m to the NW. The lateral juxtaposition of the Vernar member with the Uggowitz Breccia Formation in the SE part of the exposure (Fig. 2) implies the existence of a steep NW-dipping synsedimentary normal fault separating these two units, which is presently covered by scree. This fault must have formed after the deposition of the Vernar member but terminated its activity before the end of the deposition of the Uggowitz Breccia Formation, as the prominent topmost breccia layer

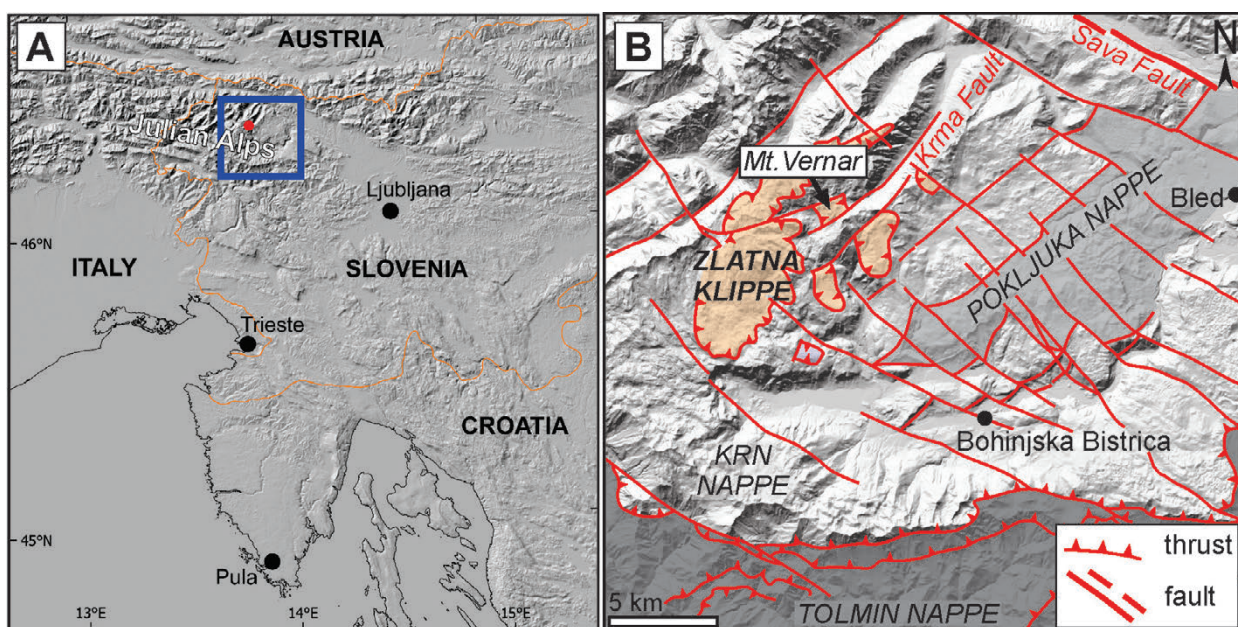


Figure 1. Location of the study area. **A:** Geographical position of the Julian Alps and of the study area (shown by a red dot). The blue rectangle indicates the map area shown in Fig. 1B. **B:** Simplified tectonic map of the eastern Julian Alps (after GORIČAN et al., 2018). Data sources: EU-DEM digital elevation model (produced using Copernicus data and information funded by the European Union), Europe coastline shapefile (European Environmental Agency), and digital elevation model with 5 × 5 m raster grid, DEM 5, 2006 (Public Information of Slovenia, The Surveying and Mapping Authority of the Republic of Slovenia).

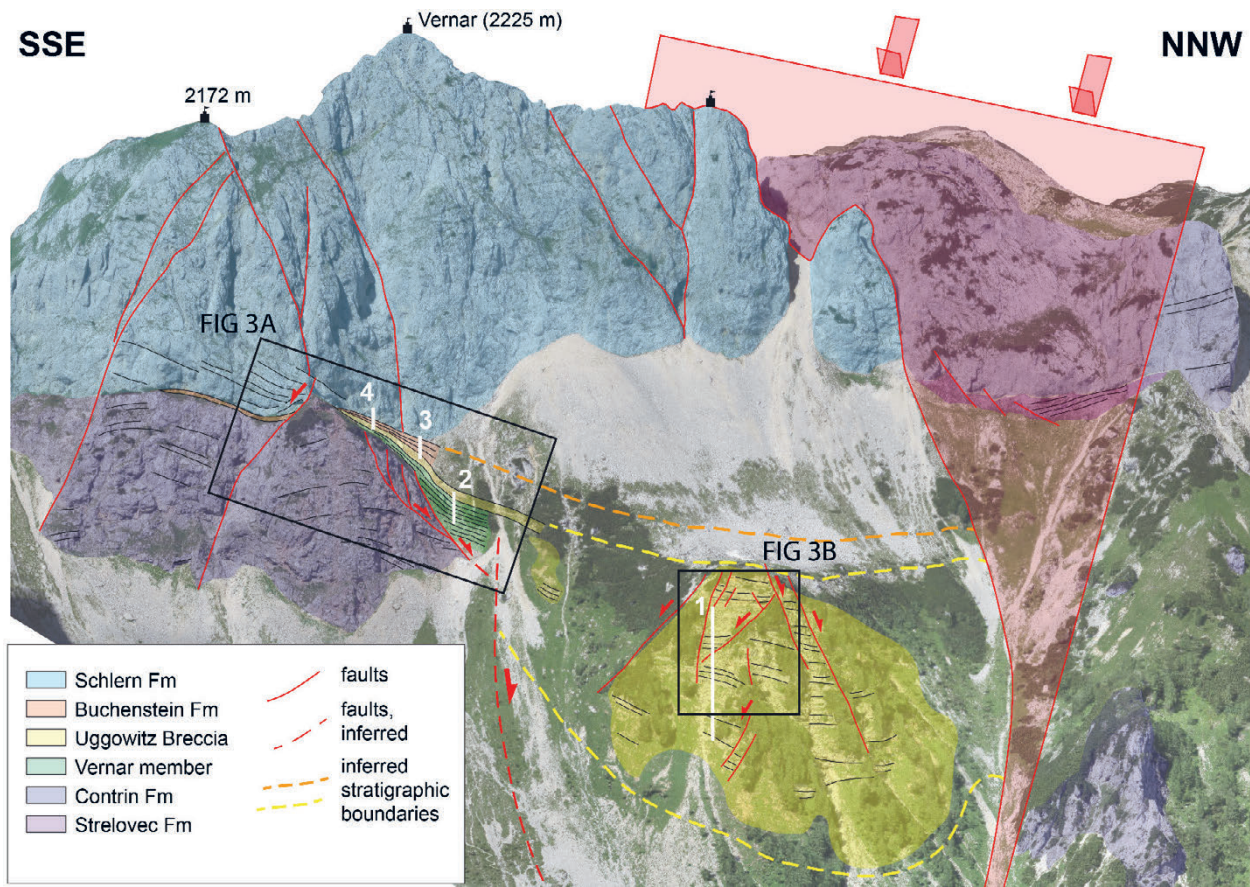


Figure 2. Oblique aerial view of the ENE face of Mt. Vernar, showing the interpreted geometry of the stratigraphic formations and structures described in this work (image produced from the photogrammetrically-generated 3D model). The locations of the logged sections described in the text are also shown.

is not transected (Fig. 2). Breccia beds and subordinate beds and lenses of sandstone in the larger outcrop are cut by numerous small-scale conjugate normal faults (Fig. 3B). The faults strike NE-SW and dip towards the SE and NW at around 60°.

The Uggowitz Breccia Formation is vertically succeeded by approximately 7 m of bedded sandy limestone and sandstone which we attribute to the Buchenstein Formation. The outcrop of the Buchenstein Formation is very limited and its NW-ward con-

tinuation is only speculative due to extensive cover by scree deposits (Fig. 2). Immediately NW-ward of our study area, green tuff layers also outcrop (Fig. 2).

The Buchenstein Formation is followed by weakly and discontinuously bedded limestone, which passes upwards into the massive limestone of the Schlern Formation (Figs. 2, 3A).

The pre-Schlern succession is terminated to the NNW by a NE-SW-striking fault with a ~30 m wide fault zone, which forms

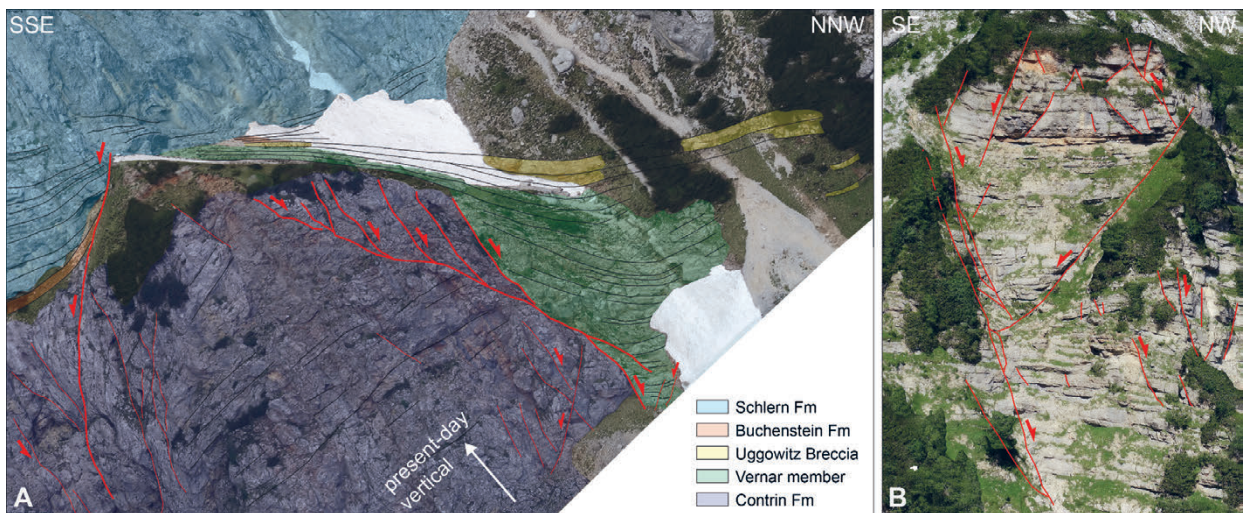


Figure 3. Detailed views of the geological structure of the ENE slope of Mt. Vernar in the photogrammetrically-generated 3D model. Refer to Fig. 2 for locations. **A:** View of the SE part of the exposure, showing the pinching out of beds and the normal fault controlling the deposition of the Vernar member. Field of view is rotated to better visualize the original depositional geometry. **B:** Conjugate SE-NW-striking, probably syndimentary normal faults and fractures cutting the Uggowitz Breccia Formation. Vertical extent of the field of view is approximately 90 m.

a prominent narrow gully in the northern ridge of Mt. Vernar and dips 65°–70° towards the SE. We interpret this fault as the master fault of the Middle Triassic half-graben. The somewhat curved trace of the master fault in map view suggests that it may have a listric geometry with the dip angle decreasing downdip, but this is not clearly visible in the field. On the NNW side of the master fault a few tens of metres of thin-bedded marly limestone, dolostone and marlstone of the (middle?) Anisian Strelovec Formation are exposed below the basal part of the massive limestone of the Contrin (?) Formation.

4.2. Description of the lithological units

The succession on the NE slope of Mt. Vernar was logged in four sections, graphically presented in Figure 4.

The Vernar member was recorded in the lower 15 m of section 2 (Fig. 4). Pinkish limestone is divided into beds 5–15 cm thick, amalgamated in “packages” ranging in thickness from 20 cm to 100 cm (Fig. 5A). Some beds are crosscut by neptunian dykes some dm thick, filled with breccia, which is identical in appearance to the breccias described from the Uggowitz Breccia Formation (Fig. 5B). The limestone is fenestral microbialite boundstone (Fig. 5C, F) and wackestone/packstone. Microbialite boundstone (locally representing up to 50% of the rock volume) comprises clumps of peloidal micrite and structureless leiolite. Birdseye fenestrae are mostly irregular in shape, a few mm in size, and in some thin sections represent up to 50% of the sample. Some are geopetally filled with sediment and cement in the following order: (1) micrite, (2) silt-sized micrite with rare ostracod valves, (3) acicular/fibrous rim cement, with (4) crystal silt and blocky spar filling the remaining space. Ostracods with both valves and foraminifers can be found in some of the cement-filled fenestrae. The wackestone/packstone locally represents up to 50% of the samples. It contains small pellets, ostracods with disarticulated or complete carapaces, foraminifers (common *Endotriada* sp., *Earlandia* sp., *Krikoumbilica* sp., rarely small *Fronicularia* sp., *Reophax* sp., *Endotabanella* or *Ammobaculites* sp., and some undetermined involutinids – see Fig. 5D), *Tubiphytes/Schamovella*-like microproblematica, calcimicrobes in growth positions (Fig. 5E), and sporadically also echinoderms and gastropods.

The Vernar member is followed by the Uggowitz Breccia Formation. The latter was recorded in Section 1 (separated from the wall by scree deposits) in a total thickness of 65 m, whereas it is only a few metres thick in other sections (Fig. 4). The Uggowitz Breccia Formation is predominantly represented by clast-supported breccia (Fig. 6). Thinner (5–15 cm) beds and lenses of carbonate sandstone and mudstone occur subordinate to the breccia beds. Breccia beds are 0.2–5 m thick (Fig. 6A). Bed boundaries are irregular, with clasts often protruding from the upper bedding plane (Fig. 6B). Several beds display internal layers, which are in some cases normally or inversely graded (Figs. 6C–D). Clasts are poorly sorted, ranging in size from 0.5 cm to 0.5 m. They often represent up to 90% of the rock, strongly dominating over the matrix. Clasts are sub-rounded to angular, with sutured, long, and concavo-convex, more rarely tangential contacts. Between 55% and 95% of clasts are represented by lithoclasts of carbonate rocks (Fig. 7A), light and dark grey in colour, or with pink, red, or yellow hues that can be divided into several groups. The most common microfacies of the carbonate clasts is calcimudstone (Group A). Group B includes common lithoclasts of grainstone to rudstone with bioclasts and lithoclasts of microbialite (Fig. 7B), fenestral peloid grainstone (microbialite), and ho-

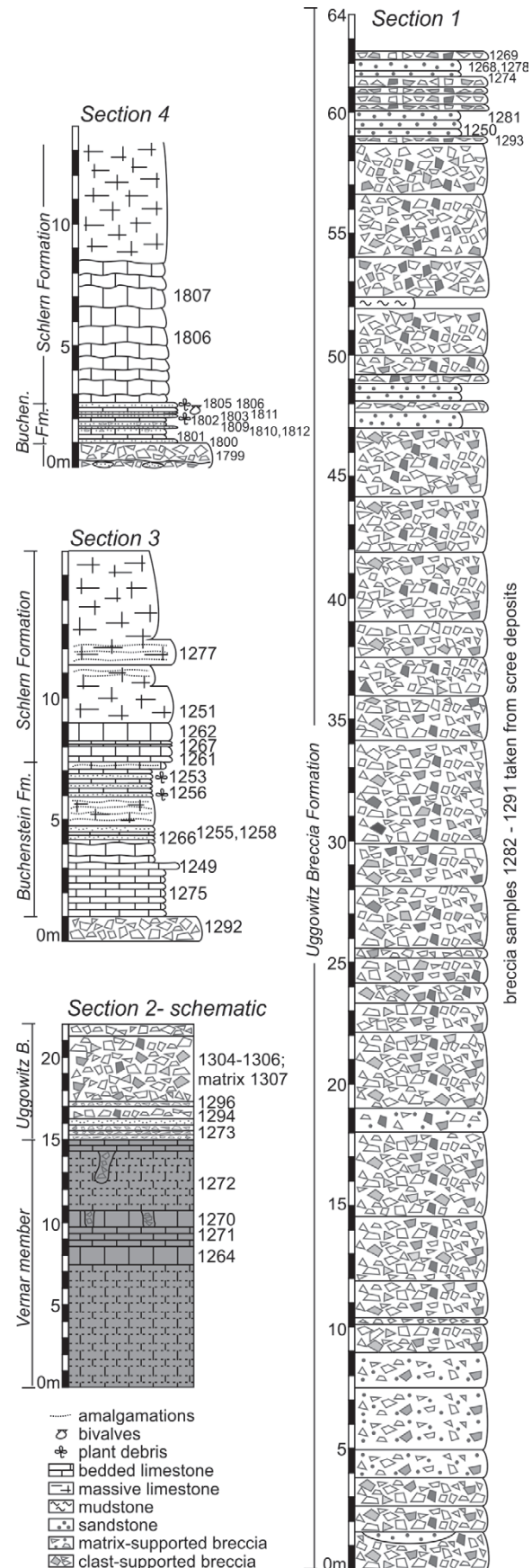


Figure 4. Logged sections. Note that the distribution of the sections in this figure does not correspond to their stratigraphic order or their lateral relationships. See Figure 2 for locations. Section coordinates (obtained with GNSS in WGS 84, September 2019): Section 1: lat. 46°21'47.46", long. 13°51'56.14". Section 2: lat. 46°21'41.98", long. 13°51'50.91". Section 3: lat. 46°21'41.98", long. 13°51'50.17". Section 4: lat. 46°21'40.59", long. 13°51'47.94".

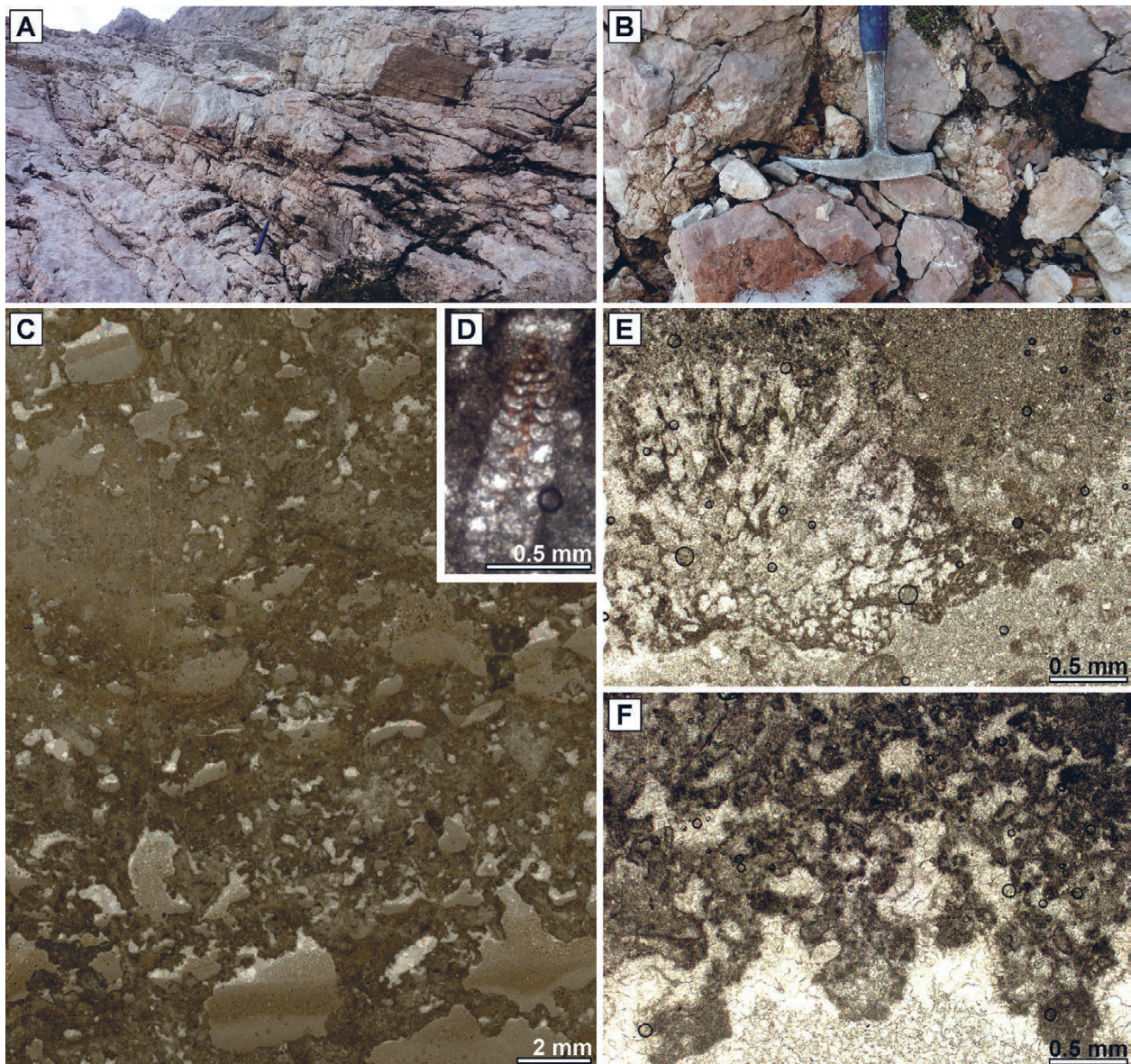


Figure 5. Field view and photomicrographs of the Vernar member. **A:** Field photo of the pinkish nodular limestone. **B:** Neptunian dyke cutting the pinkish nodular limestone and filled with breccia. **C:** Fenestral microbialite boundstone. Thin section 1264. **D:** Undetermined aragonitic foraminifer. Thin section 1270. **E:** Calcimicrobe in growth position. Thin section 1272. **F:** Pelletal grainstone (microbialite) with fenestrae. Thin section 1272.

mogenous or laminated microbialite boundstone (leiolite and stromatolite). The common bioclasts are *Tubiphytes/Schamovella*-like microproblematica (including *Tubiphytes/Schamovella* sp. and *Plexoramea* sp.), and cortoids. Less common are ostracods, brachiopods, bivalves, echinoderms, foraminifers, and dasycladacean algae. The foraminiferal assemblage within the clasts of Group B consists of *Citaella dinarica* (Kochansky-Devidé and Pantić) (Fig. 7D–E), *Pilammina semiplana* (Kochansky-Devidé and Pantić) (Fig. 7F), and *Endotriadella wirzi* (Koehn-Zaninetti) (Fig. 7G). Completely recrystallised limestone represents the clasts of Group C, which is next in terms of abundance. Less common are the lithoclasts of Group D, comprising fenestral peloid-bioclastic packstone, peloid-bioclastic wackestone, peloid packstone, and peloid wackestone with a partly washed matrix. Rare clasts of foraminiferal wackestone (Group E) contain a high density of the foraminifer *Pilamina densa* Pantić (Figs. 7H). Fenestral calcimudstone or sparse wackestone with some foraminifers and ostracods (Group F), together with filament wackestone, and radiolarian wackestone to packstone (Fig. 7C) (Group

G) are very rare among carbonate clasts. Subordinate to limestone clasts are clasts of red rhyolite, red, and greenish grey peperite, green tuff, light brown, beige and red sandstone, mudstone, and clasts of fault breccias. The breccia matrix is sandy, locally muddy, and represents only 10–30% of the rock. It is commonly reddish orange in colour, locally greenish grey. It locally consists of up to 50% grains of quartz, feldspar (plagioclase), and some opaque minerals.

Beds and lenses of sandstone and mudstone are subordinate to the breccia beds, and are between 5 cm and 15 cm thick. Mudstone commonly contains small coalified fragments of terrestrial plants. Sandstone is fine- to coarse-grained. A few beds show boundary-parallel (horizontal) planar lamination (Fig. 8A). Sand particles are poorly to moderately sorted, with point, long, concavo-convex, and, in some samples, sutured contacts (Fig. 8B). Approximately 90% of clasts are carbonate lithoclasts, which texturally match the prevailing carbonate clasts described from breccias (see above). Quartz, mica, plagioclase, and opaque minerals, as well as clasts of volcanic rocks and mudstone are

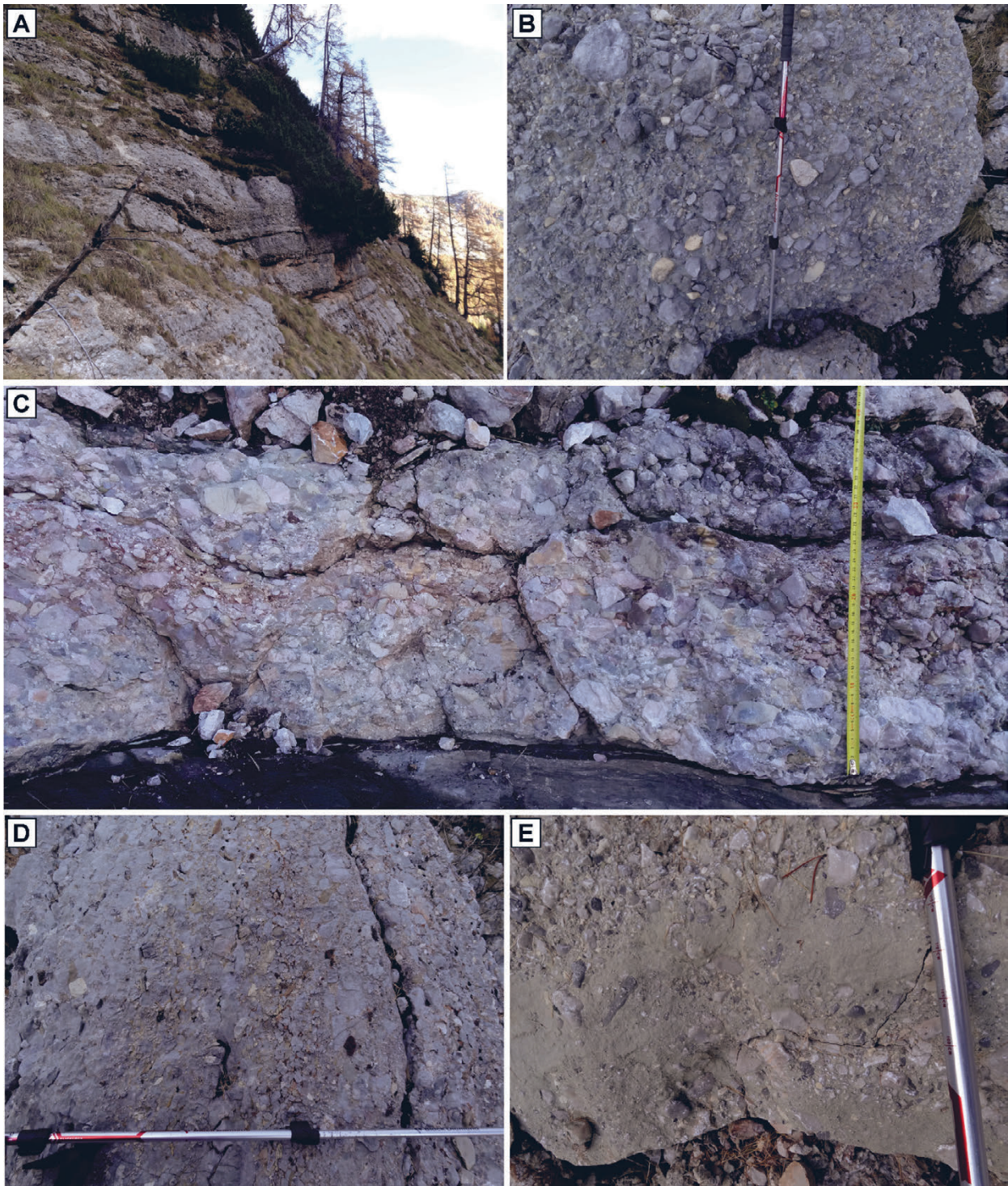


Figure 6. Field aspect of breccia within the Uggowitz Breccia Formation. **A:** Well-expressed bedding. Beds are laterally continuous. **B:** Upper surface of the breccia bed. Note the clasts protruding from the upper bed surface, characteristic of the debris flow deposits. **C:** Amalgamation (along the irregular line) of two (or more) layers of breccia. **D:** Stacking of several inversely or normally graded layers of breccia (block rotated by 90° with respect to the bedding). **E:** Rare example of matrix-supported breccia.

present in subordinate amounts. The matrix (10–40% of the rock volume) is micrite or microsparite, locally limonitic.

The uppermost breccia bed shows transitions from a red, to green-grey, and finally an almost black coloured matrix. The clasts in these beds are less variable in lithology, represented only by white, grey, beige, and pink limestone, and lacking clasts of volcanic and volcanoclastic rocks.

The Buchenstein Formation overlying the Uggowitz Breccia Formation consists of thin beds of dark brown sandstone and

sandy limestone, which often contains coalified plant fragments. The sandstone beds range from 4 cm to 20 cm in thickness. The sandstone is moderately to well sorted (Fig. 9a). Depending on the amount of micritic carbonate matrix, grains are in point or long contacts. Angular carbonate lithoclasts predominate: micritic and microsparitic clasts represent 50% of all clasts, and an additional 12% of clasts are completely recrystallised limestone. Clasts of volcanoclastic rocks, quartz, feldspar, and of undetermined opaque minerals represent 35% of clasts. Bioclasts, such

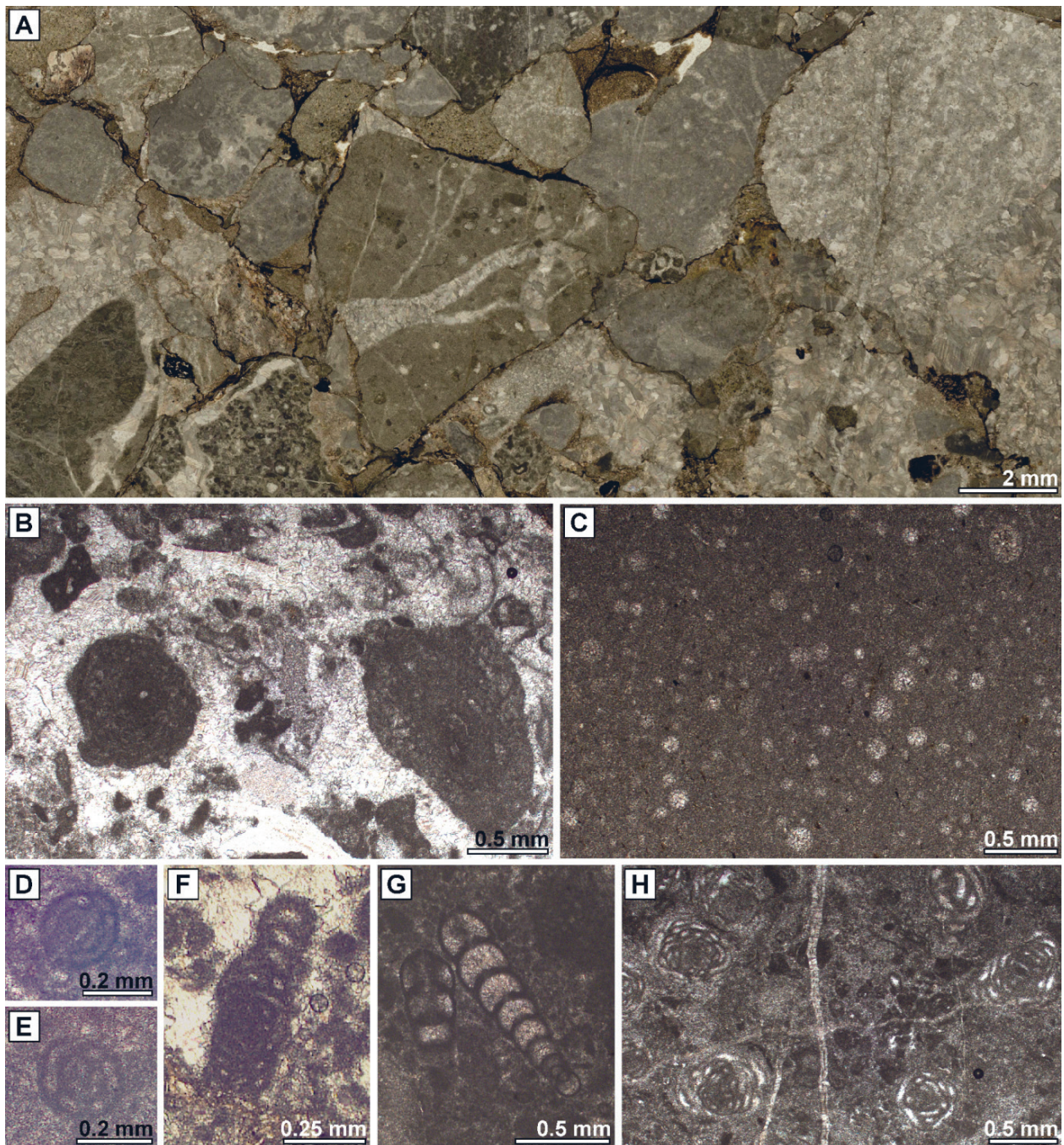


Figure 7. Clast composition within the Uggowitz Breccia Formation with some important microfacies types and microfossils. **A:** Grain-supported fabric and poly-mict clasts. Thin section 1303a. **B:** Grainstone with bioclasts and microbialite intraclasts. The two largest grains are *Tubiphytes/Schamovella*-like microproblematica. Clast from breccia. Thin section 1304. **C:** Clast of radiolarian wackestone to packstone. Thin section 1293. **D–E:** *Citaella dinarica* (Kochansky-Devidé and Pantić) within a clast. Off-centred section. Thin section 1288. **F:** *Pilammina semiplana* (Kochansky-Devidé and Pantić) within a clast. Thin section 1297. **G:** *Endotriadella wirzi* (KoeHN-Zaninetti) within a clast. Thin section 1293. **H:** *Pilamina densa* Pantić within a clast. Thin section 1304.

as bivalve and brachiopod shells, gastropods, ostracods, foraminifers, and echinoderms are rare, or are only locally more abundant. Some sandstone beds also contain centimetre-sized lithoclasts (Fig. 9B). Limestone and sandy limestone beds are 15–25 cm thick. Microfacies types include calcimudstone, laminated calcimudstone, and peloid wackestone, peloid packstone with partly washed matrix (Fig. 9C), bioclastic-intraclastic packstone (Fig. 9D–E), wackestone with *Tubiphytes/Schamovella*-like microproblematica (Fig. 9F), and oncoid rudstone. The calcimudstone locally contains a small admixture of silt-sized terrigenous material, pellets, and a few bioclasts (echinoderms, foraminifers, ostracods). In addition to peloids, the peloid packstone with partly

washed matrix contains subordinate bivalves, foraminifers (?*Trochammina* sp., *Glomospirella* sp., and Endothyraea), echinoderms, gastropods, and ostracods, as well as small amounts of fine grains of quartz, feldspar, and volcanics. The bioclastic-intraclastic packstone is relatively rich in foraminifers (Fig. 10). Involutinidae *Parvalamella friedli* (Kristan-Tollmann) and ?*Aulotortus? eotriasicus* Zaninetti, Rettori and Martini, as well as Duostominoidea are abundant and well preserved. The specimens determined as ?*Aulotortus? eotriasicus* Zaninetti, Rettori, and Martini are somewhat smaller than the holotype and the paratypes (0.8–1.6 mm in diameter, according to ZANINETTI et al., 1994), and display glomospiral initial coiling, whereas only small

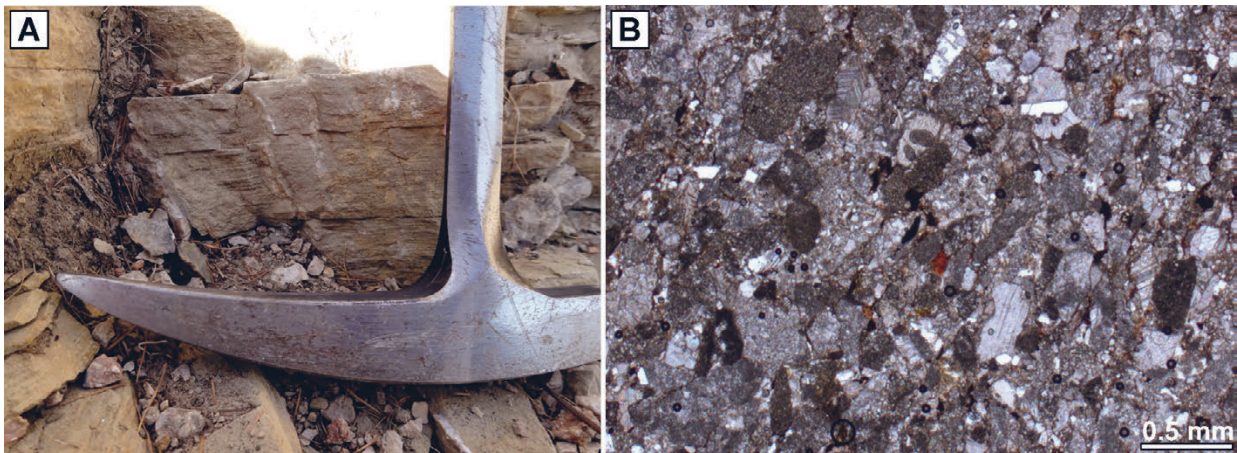


Figure 8. Field view and microfacies of sandstone. **A:** Parallel horizontal lamination. **B:** Photomicrograph of sandstone from the Uggowitz Breccia Formation. Thin section 1300.

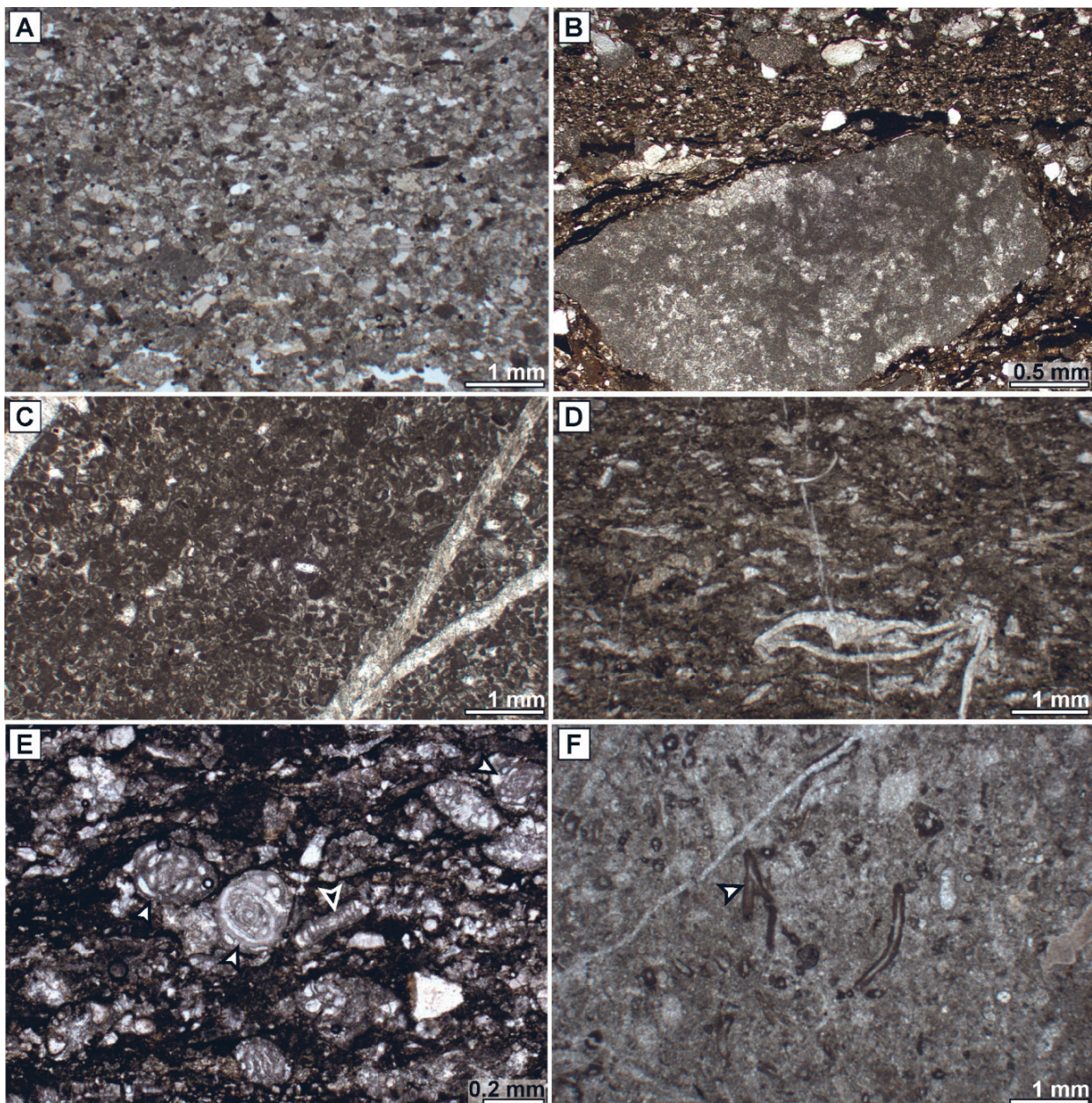


Figure 9. Microfacies of the Buchenstein Formation. **A:** Sandstone. Thin section 1256A. **B:** Large lithoclast in sandstone. Thin section 1802. **C:** Partly washed peloid packstone. Thin section 1801. **D:** Bioclastic-intraclastic packstone. Thin section 1275. **E:** Bioclastic-intraclastic packstone. The white arrowhead points to *Parvalamella friedli* (Kristan-Tollmann). The black arrowhead with white outline points to *Aulosina* sp. Thin section 1266. **F:** Wackestone with *Tubiphytes/Schamovella*-like microproblematica (arrowhead). Thin section 1253.

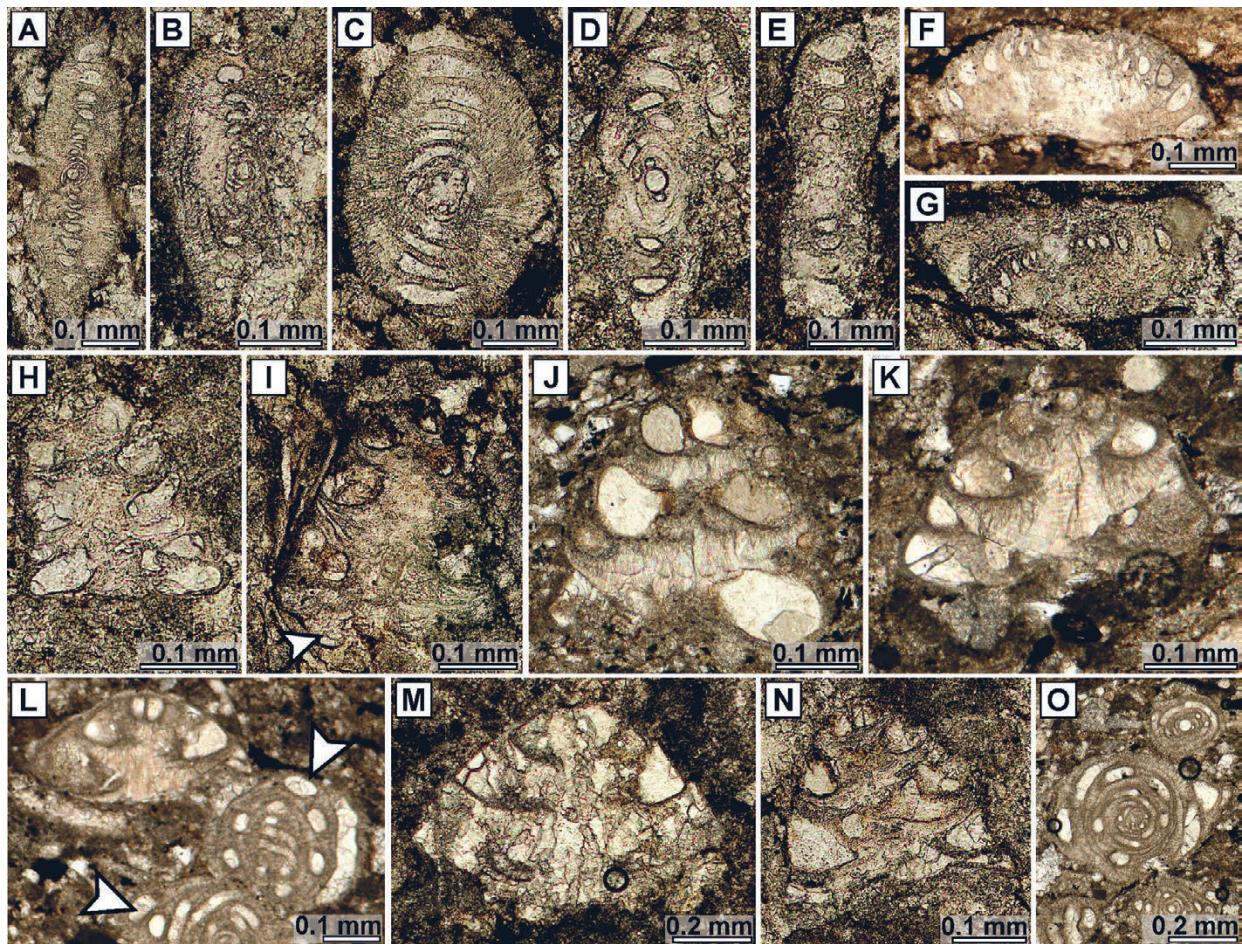


Figure 10. Foraminifers from the Buchenstein Formation. Thin sections, not shown in Fig. 4, are cut from samples collected from the scree deposit. Foraminifera from these samples are illustrated here solely because of their good preservation. **A-C:** *?Aulotortus? eotriasicus* Zaninetti et al. Note that some specimens appear biconcave due to stylolitization. Thin sections: 1266 (figs. A, C), 1255 (fig. B). **D-E:** *?Aulosina* sp. Thin sections 1255 (fig. D), 1266 (fig. E). **F-G:** *Lamelliconus* ex gr. *ventroplanus* (Oberhauser) sensu RETTORI (1995). Thin section 1266 (fig. F). Specimen in figure G is from the sample from scree. **H-I:** *?Trocholina* cf. *turris* Frentzen. Note the papillae in the umbilical mass (arrowhead) in fig. I. Thin sections: 1255 (fig. H), 1266 (fig. I). **J-K:** *?Duostominidae*. Sample from scree. **L:** *Duostomina biconvexa* Kristan-Tollmann. Arrowheads point to *Parvalamella friedli* (Kristan-Tollmann). Sample from scree. **M:** *Duostomina alta* Kristan-Tollmann. Thin section 1258. **N:** *?Diplotremina altoconica* Kristan-Tollmann. Thin section 1266. **O:** *Parvalamella friedli* (Kristan-Tollmann). Sample from scree.

deviations from the planispiral coiling have been observed in the type material of this species (ZANINETTI et al., 1994). The biconcave shape of some specimens (e.g., Figs. 10A, D) is probably due to stylolitization and is not a primary characteristic of them. Other important species from this microfacies include *Lamelliconus* ex gr. *ventroplanus* (Oberhauser) sensu (RETTORI, 1995), *?Aulosina* sp., and *?Trocholina* cf. *turris* Frentzen. Other bioclasts present include bivalve shells, echinoderms, gastropods, ostracods, and *Tubiphytes/Schamovella*-like microproblematica. Some limestone beds become progressively sandier towards the top, and a few end with a horizon of mud-supported breccia. One limestone bed was found to hold small, disarticulated bivalves on the upper bedding plane.

Transition from the Buchenstein Formation to the Schlern Formation is through several beds 25–80 cm thick in total thickness of 6 m. Light grey limestone is texturally poorly sorted bioclastic wackestone (Fig. 11A), intraclastic-bioclastic grainstone, and oncoid rudstone (Fig. 11B,C). The wackestone contains corals, echinoderms, bryozoans, gastropods, bivalves, ostracods, and foraminifers (*?Ammobaculites* sp., Endothyraea, *Trochammina almtalensis* Koehn-Zaninetti). Micritic intraclasts predominate in the intraclastic-bioclastic grainstone. Thalamid and other sponges, *Tubiphytes/Schamovella*-like microproblematica, dasycladacean algae (Fig. 11D), bivalves, echinoderms, foraminifers,

and ostracods are present. Foraminifers include *Ammobaculites* sp. or *Endotebanella* sp. (“*Earlandinita oberhauseri* Salaj” = “*Earlandinita elongata* Salaj” in SALAJ et al. 1967) (Fig. 11E), *Reophax* sp., Endothyraea, *Endotriadella wirzi* (Koehn-Zaninetti) (Fig. 11F), “*Tetrataxis*” *nanus* Kristan, and Duostominoidea. Massive limestone prevails upwards forming near-vertical walls that could not be sampled in situ.

5. DISCUSSION

We interpret the structure of the NE slope of Mt. Vernar as a Middle Triassic half-graben with its sediment infill thickening North-westward towards the NE-SW-striking master fault and pinching out towards the SE edge of the half-graben (Fig. 2). The master fault was also (re)activated after the sedimentation of the Anisian Mt. Vernar succession, as a significant vertical slip can be determined from the elevated position of the Contrin (?) Formation on the other side of the master fault. From the consistent NE-SW strike of the bounding faults and of the conjugate extensional faults and fractures within the half-graben we conclude that the half-graben formed during NW-SE oriented extension (in present-day reference frame).

The recorded succession is comparable, though not completely identical to some other examples of graben-filling succes-

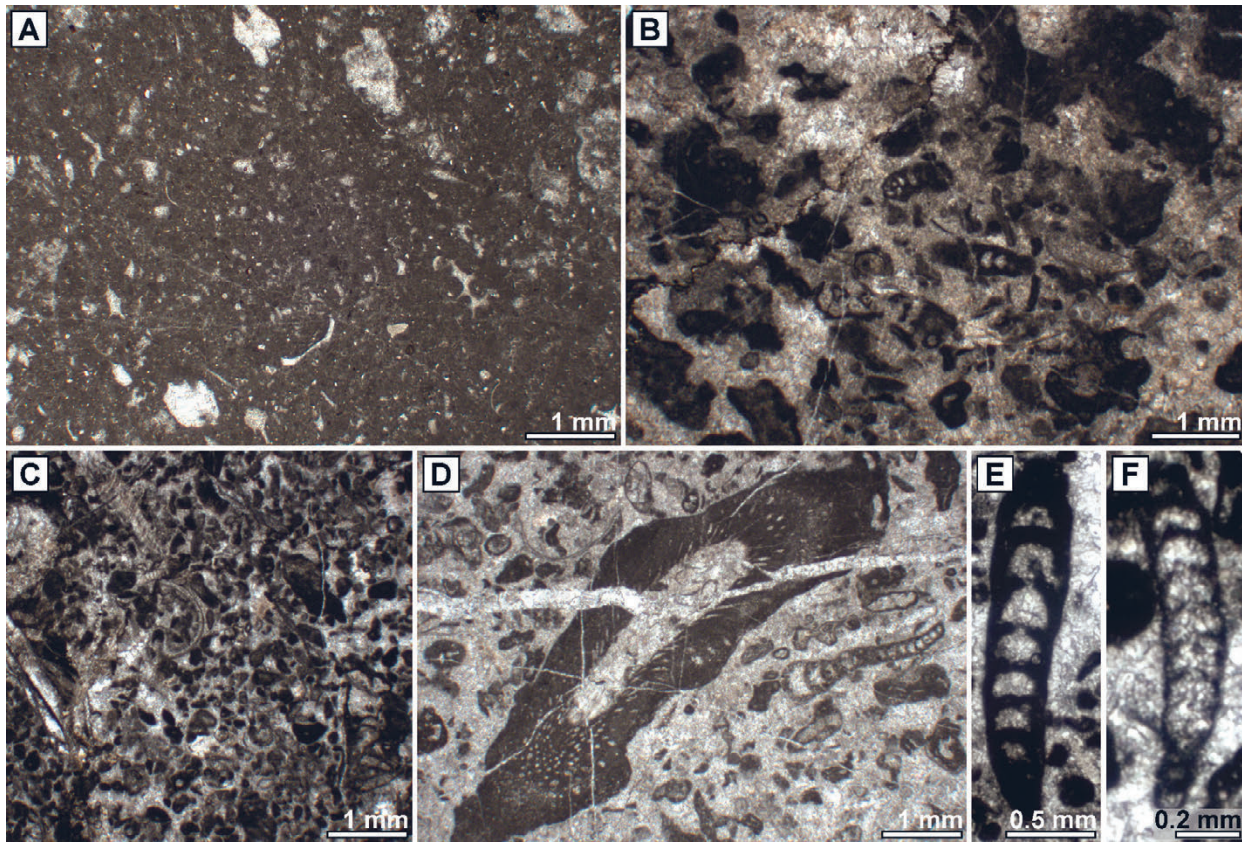


Figure 11. Microfacies of the Schlern Formation. **A:** Bioclastic wackestone. Thin section 1807. **B:** Intraclastic-bioclastic grainstone. Thin section 1251. **C:** Intraclastic-bioclastic grainstone. Thin section 1261. **D:** Dasycladacean algae in intraclastic-bioclastic grainstone. Thin section 1262. **E:** *Ammobaculites* sp. or *Endotabanella* sp. ("*Earlandinita oberhauseri* Salaj" = "*Earlandinita elongata* Salaj" in SALAJ et al., 1967). Thin section 1267. **F:** *Endotriadella wirzi* (Koehn-Zaninetti). Thin section 1267.

sions from the Julian and the Kamnik-Savinja Alps occurring within the late Anisian–early Ladinian time interval (CELARC et al., 2013). The most notable difference is that the Uggowitz Breccia Formation on the slopes of Mt. Vernar is not underlain by the radiolarian-rich Loibl Formation. Instead, the limestone of the Vernar member below the Uggowitz Breccia Formation is riddled with fenestrae, which seem to be either constructional or are the product of early diagenesis (the late diagenetic origin of fenestrae can be excluded based on ostracods found within the micrite filling the fenestrae). Based on the presence of calcimicrobes in growth position, we suggest that deposition still took place within the photic zone. The normal fault zone between the massive limestone of the Contrin (?) Formation and the Vernar member indicates formation of a shallower basin, filled with the nodular limestone prior to formation of the much steeper fault and deposition of the Uggowitz Breccia Formation. The timing of the deposition of the Uggowitz Breccia Formation has to be estimated on the basis of superposition and/or the age of the youngest clasts found in the breccia. Whereas most limestone clasts with fossils are middle to late Anisian in age (based on the foraminifera *Citaella dinarica*, *Pilamminella semiplana*, *Endotriadella wirzi*, and *Pilamina densa*; see RETTORI, 1995), the limestone clasts with radiolarians and filaments probably originate from the Loibl Formation, which has been dated in the Kamnik-Savinja Alps to the Illyrian (KOLAR-JURKOVŠEK, 1983; PETEK, 1998; BUSER et al., 2008; CELARC et al., 2013). Based on these clasts, the Uggowitz Breccia below Mt. Vernar was most likely deposited during the Illyrian or somewhat later. This is in accordance with the sequence chronostratigraphic scheme for the

northern Julian Alps by GIANOLLA et al. (1998), and previous research by CELARC et al. (2013).

The large proportion of clasts (up to 90% of the rock volume), their poor sorting, the presence of internal layering, inverse and normal grading, and especially the irregular nature of the upper bedding planes, which are studded by protruding clasts, suggests that breccias within the Uggowitz Breccia Formation are debris flow deposits (SOHN, 2000; PROTHERO & SCHWAB, 2013). The internal layering observed within the individual beds of breccia results from the stacking of several debris-flow surges (SOHN, 2000). The subordinate beds of sandstone were probably deposited by turbidity currents generated by flow transformation of the gravelly debris flow (MOHRIG et al., 1998; SOHN, 2000). The deposition of the Uggowitz Breccia Formation within a submerged half-graben fits either the coastal marine gulf basin or the coastal/shelf basin with carbonate facies model, or both, since the first can evolve into the latter (LEEDER & GAWTHORPE, 1987). According to the coastal marine gulf and coastal/shelf basins, breccias represent footwall submarine fans and/or peri-platform talus generated through slumping and debris flow mechanisms.

The Buchenstein Formation of the logged section was also deposited in a marine environment, as evidenced by the common presence of foraminifers and echinoderms. We interpret these clasts as redeposited material of shallower origin. Bioclasts of shallow-marine origin, most notably dasycladacean algae and corals, also predominate within the Buchenstein Formation in half-grabens previously documented by CELARC et al. (2013). The concomitant occurrence of terrestrial plant fragments and sandy terrigenous material suggests close proximity to the coast,

although small plant fragments may be transported far from the shore either as floating material or via turbidity currents. Lenses and thin tongues of pebble to cobble size clasts in some limestone beds could represent terminations of lower-viscosity debris flows in a subaqueous environment (NEMEC & STEEL, 1984).

The Schlern Formation formed as a carbonate platform under subtidal conditions and is free from terrigenous input. This suggests a migration of the coastline landwards and the relative rise of sea level. Recorded foraminifera are of insufficient stratigraphic resolution or have insufficiently defined timespans to determine their precise age. According to GIANOLLA et al. (1998) and MIETTO et al. (2020), the base of the Schlern Formation is latest Illyrian to Fassanian in age.

6. CONCLUSIONS

The stratigraphic succession below Mt. Vernar in the Julian Alps represents a sedimentary fill of a half-graben formed during crustal extension at the end of the Anisian. The beginning of extension is marked by the formation of a low-angle normal fault zone and deposition of the Vernar member, filling the newly created basin and stepping over the fault scarp. The deposition of the Vernar member probably took place within the photic zone. Following deposition of the Vernar member, a steeper fault created a deeper half-graben extending in the present-day NE–SW direction. The sedimentary infill of this half-graben comprises the Uggowitz Breccia Formation and the Buchenstein Formation. The latter is overlain by the prograding carbonate platform of the Schlern Formation. The recorded succession is similar to previously recorded examples from the Kamnik-Savinja Alps, the Julian Alps, the Karavanke Mts., and the External Dinarides, where the Uggowitz Breccia Formation is under- and overlain by platform carbonates. The Uggowitz Breccia from the Carnic Alps, in contrast, was deposited on top of a more substantial unconformity and is instead interpreted as a fluvial or paralic deposit, forming the base of a new transgression.

ACKNOWLEDGEMENT

This research was financially supported by the Slovenian Research Agency (research core funding No. P1-0011 to L.G. and B.C. and No. P1-0195 to M.V.). We thank the technical staff of the Geological Survey of Slovenia for the preparation of thin sections. We particularly thank the reviewers for their suggestions and useful comments, which helped us in our interpretation of the field data.

REFERENCES

- BALINI, M., JURKOVŠEK, B. & KOLAR-JURKOVŠEK, T. (2006): New Ladinian ammonoids from Mt. Svilaja (External Dinarides, Croatia).— *Riv. Ital. Palaeont. Stat.*, 112, 383–395. doi: 10.11310/2039-4942/6348
- BERRA, F. & CARMINATI, E. (2010): Subsidence history from a backstripping analysis of the Permo-Mesozoic succession of the Central Southern Alps (northern Italy).— *Basin Res.*, 22, 952–975. doi: 10.1111/j.1365-2117.2009.00453.x
- BOSELLINI, A., GIANOLLA, P. & STEFANI, M. (2003): Geology of the Dolomites.— *Episodes*, 26, 181–185. doi: 10.18814/epiugs/2003/v26i3/005
- BUDAI, T. & VÖRÖS, A. (2006): Middle Triassic platform and basin evolution of the Southern Bakony Mountains (Transdanubian Range, Hungary).— *Riv. It. Palaeont. Strat.*, 112, 359–371. doi: 10.11310/2039-4942/6346
- BUSER, S. (1989): Development of the Dinaric and the Julian carbonate platforms and of the intermediate Slovenian Basin (NW Yugoslavia).— *Boll. Soc. Geol. Ital.*, 40, 313–320.
- BUSER, S., KOLAR-JURKOVŠEK, T. & JURKOVŠEK, B. (2008): The Slovenian Basin during the Triassic in the light of conodont data.— *Boll. Soc. Geol. Ital.*, 127, 257–263.
- CAPUTO, R., POLI, M.E. & ZANFERRARI, A. (2010): Neogene–Quaternary tectonic stratigraphy of the eastern Southern Alps, NE Italy.— *J. Struct. Geol.*, 32, 1009–1027. doi: 10.1016/j.jsg.2010.06.004
- CASTELLARIN, A. & CANTELLI, L. (2000): Neo-Alpine evolution of the Southern Eastern Alps.— *J. Geodyn.*, 30, 251–274. doi: 10.1016/S0264-3707(99)00036-8
- CELARC, B., GORIČAN, Š. & KOLAR-JURKOVŠEK, T. (2013): Middle Triassic carbonate-platform break-up and formation of small-scale half-grabens (Julian and Kamnik-Savinja Alps, Slovenia).— *Facies*, 59, 583–610. doi: 10.1007/s10347-012-0326-0
- DUNHAM, R.J. (1962): Classification of carbonate rocks according to depositional texture.—In: HAN, W.E. (ed.): *Classification of carbonate rocks, A symposium*. Amer. Ass. Petrol. Geol. Mem., 108–121. doi: doi.org/10.1306/M1357
- EMBRY, A.F. & KLOVAN, J.E. (1971): A late Devonian reef tract on northeastern Banks Island.— *NWT Bull. Can. Petrol. Geol.*, 19, 730–781.
- FARABEGOLI, E. & LEVANTI, D. (1982): Triassic stratigraphy and microfacies of the Monte Pleros (Western Carnia, Italy).— *Facies*, 6, 37–58.
- FARABEGOLI, E., JADOUL, F. & MARTINES, M. (1985): *Stratigrafia e Palaeogeografia anisiche delle Alpi Giulie occidentali (Alpi Meridionali – Italia)*.— *Riv. It. Palaeont. Strat.*, 91, 147–196.
- GAWLICK, H.-J., GORIČAN, Š., MISSONI, S. & LEIN, R. (2012): Late Anisian platform drowning and radiolarite deposition as a consequence of the opening of the Neotethys ocean (High Karst nappe, Montenegro).— *Bull. Soc. géol. France*, 183, 349–358. doi: 10.2113/gssgfbull.183.4.349
- GIANOLLA, P., DE ZANCHE, V. & MIETTO, P. (1998): Triassic sequence stratigraphy in the Southern Alps (Northern Italy): definition of sequences and basin evolution.— In: DE GRACIANSKY, P.C., HARDENBOL, J., JACQUIN, T. & VAIL, P.R. (eds): *Mesozoic and Cenozoic Sequence Stratigraphy of European Basins*.— *SEPM Spec. Publ.*, 60, 719–746. doi: 10.2110/pec.98.02.0719
- GORIČAN, Š., KOŠIR, A., ROŽIČ, B., ŠMUC, A., GALE, L., KUKOČ, D., CELARC, B., ČRNE, A.E., KOLAR-JURKOVŠEK, T., PLACER, L. & SKABERNE, D. (2012): Mesozoic deep-water basins of the eastern Southern Alps (NW Slovenia).— *J. Alpine Geol.*, 55, 1–43.
- GORIČAN, Š., ŽIBRET, L., KOŠIR, A., KUKOČ, D. & HORVAT, A. (2018): Stratigraphic correlation and structural position of Lower Cretaceous flysch-type deposits in the eastern Southern Alps (NW Slovenia).— *Int. J. Earth Sci.*, 107, 2933–2953. doi: 10.1007/s00531-018-1636-4
- GORIČAN, Š., HORVAT, A., KUKOČ, D. & VERBIČ, T. (2022): Stratigraphy and structure of the Julian Alps in NW Slovenia.— *Folia Biolog. Geolog.*, 63, 61–83. doi: 10.3986/fbg0098
- HAAS, J. & BUDAI, T. (1999): Triassic sequence stratigraphy of the Transdanubian Range (Hungary).— *Geol. Carpathica*, 50, 459–475.
- HAAS, J., KOVÁCS, S., KRYSZYN, L. & LEIN, R. (1995): Significance of Late Permian–Triassic facies zones in terrane reconstructions in the Alpine–North Pannonian domain.— *Tectonophysics*, 242, 19–40. doi: 10.1016/0040-1951(94)00157-5v
- JURKOVŠEK, B. (1986): Osnovna geološka karta SFRJ 1:100000, list Beljak in Ponteba L33–52, L33–51 [*Basic Geological Map of SFRJ 1:100000, Beljak and Ponteba sheet – in Slovenian*].— Geološki zavod Ljubljana, Ljubljana, Zvezni geološki zavod, Beograd.
- JURKOVŠEK, B. (1987): Osnovna geološka karta SFRJ 1:100000. Tolmač za list Beljak in Ponteba, L33–52, L33–51 [*Basic Geological Map of SFRJ 1:100000, Geology of the Beljak and Ponteba sheet – in Slovenian*].— Geološki zavod Ljubljana, Ljubljana, Zvezni geološki zavod, Beograd, 58 p.
- KOLAR-JURKOVŠEK, T. (1983): Srednjetrijski konodonti Slovenije.— *Rudarsko-metalurški zbornik: revija za geologijo, rudarstvo in metalurgijo*, 30, 323–364.
- KOVÁCS, S., SUDAR, M., GRĀDINARU, E., GAWLICK, H.-J., KARAMATA, S., HAAS, J., PÉRO, C., GAETANI, M., MELLO, J., POLÁK, J., ALJINVIĆ, D., OGORELEC, B., KOLAR-JURKOVŠEK, T., JURKOVŠEK, B. & BUSER, S. (2011): Triassic evolution of the tectonostratigraphic units of the Circum-Pannonian Region.— *Jb. Geol. B.-A.*, 151, 199–280.
- KOZUR, H.W., KRAINER, K. & MOSTLER, H. (1994): Middle Triassic conodonts from the Southern Karawanken Mountains (Southern Alps) and their stratigraphic importance.— *Geol. Paläont. Mitt. Innsbruck*, 19, 165–199.
- KRAINER, K. & LUTZ, D. (1995): Middle Triassic basin evolution and stratigraphy in the Carnic Alps (Austria).— *Facies*, 33, 167–184. doi: 10.1007/BF02537450
- LEEDER, M.R. & GAWTHORPE, R.L. (1987): Sedimentary models for extensional tilt-block/half-graben basins.— In: COWARD, M.P., DEWEY, J.F. & HANCOCK, P.L. (eds): *Continental extensional tectonics*.— *Geol. Soc. Spec. Publ.*, 28, 139–152. doi: 10.1144/GSL.SP.1987.028.01.11
- MIETTO, P., AVANZINI, M., BELVEDERE, M., BERNARDI, M., DALL VECCHIA, F.M., O'RAZI PORCHETTI, S., GIANOLLA, P. & PETTI, F.M. (2020): Triassic tetrapod ichnofossils from Italy: the state of the art.— *J. Mediterr. Earth Sci.*, 12, 83–134.
- MOHRIG, D., WHIPPLE, K.X., HONDZO, M., ELLIS, C. & PARKER, G. (1998): Hydroplaning of subaqueous debris flows.— *GSA Bull.*, 110, 187–394. doi: 10.1130/0016-7606(1998)110<0387:HOSDF>2.3.CO;2

- NEMEC, W. & STEEL, R.J. (1984): Alluvial and coastal conglomerates: their significant features and some comments on gravelly mass-flow deposits.– In: KOSTER, E.H. & STEEL, R.J. (eds): Sedimentology of gravels and conglomerates. Can. Soc. Petrol. Geol. Mem., 10, 1–31.
- PETEK, T. (1998): Scythian and Anisian beds in the quarry near Hrastenice and important finds of Upper Anisian fossils.– *Geologija*, 40, 119–151. doi: 10.5474/geologija.1997.006
- PLACER, L. (2008): Principles of the tectonic subdivision of Slovenia.– *Geologija*, 51, 205–217. doi: 10.5474/geologija.2008.021
- POLI, M.E. & ZANFERRARI, A. (1995): Dinaric thrust tectonics in the Southern Julian Prealps (Eastern Southern Alps, NE Italy).– In: VLAHOVIĆ, I. & VELIĆ, I. (eds): Proceedings of the first Croatian Geological Congress. Institute of Geology, Croatian Geological Society, Zagreb, 2, 465–468.
- PROTHERO, D.R. & SCHWAB, F. (2013): Sedimentary geology: an introduction to sedimentary rocks and stratigraphy.– WH Freeman and Company, New York, 575 p.
- RAMOVŠ, A. (2000): Über die Zlatnplatte sensu Kossmat, 1913, Slatna-Decke sensu Buser, 1986, Slatna-Überschiebung sensu Jurkovšek, 1987 und Triglav-Decke sensu Ramovš, 1985.– *Geologija*, 43, 109–113. doi: 10.5474/geologija.2000.010
- RETTORI, R. (1995): Foraminiferi del Trias inferiore e medio della Tetide: revisione tassonomica, stratigrafia ed interpretazione filogenetica.– *Uni. Geneve, Publ. Départ. Géol. Paléont.*, 18, 1–107.
- RIDING, R. (2000): Microbial carbonates: the geological record of calcified bacterial-algal mats and biofilms.– *Sedimentology*, 47, 179–214. doi: 10.1046/j.1365-3091.2000.00003.x
- SALAJ, J., BIELY, A. & BYSTRICKÝ, J. (1967): Trias-foraminiferen in den Westkarpaten.– *Geol. Práce*, 42, 119–136.
- SMIRČIĆ, D., ALJINOVIĆ, D., BARUDŽIJA, U. & KOLAR-JURKOVŠEK, T. (2020): Middle Triassic syntectonic sedimentation and volcanic influence in the central part of the External Dinarides, Croatia (Velebit Mts.).– *Geol. Quarterly*, 64, 220–239. doi: 10.7306/gq.1528
- SOHN, Y.K. (2000): Coarse-grained debris-flow deposits in the Miocene fan deltas, SE Korea: a scaling analysis.– *Sediment. Geol.*, 130, 45–64. doi: 10.1016/S0037-0738(99)00099-8
- STEFANI, M., FURIN, S. & GIANOLLA, P. (2010): The changing climate framework and depositional dynamics of Triassic carbonate platforms from the Dolomites.– *Palaeogeogr. Palaeoclimatol. Palaeoecol.*, 290, 43–57. doi: 10.1016/j.palaeo.2010.02.018
- VELLEDITS, F., PÉRO, C., BLAU, J., SENOWBARI-DARYAN, B., KOVÁCS, S., PIROS, O., POCSAI, T., SZÜGYI-SIMON, H., DUMITRICĂ, P. & PÁLFY, J. (2011): The oldest Triassic platform margin reef from the Alpine-Carpathian region (Aggtelek, NE Hungary): platform evolution, reefal biota and biostratigraphic framework.– *Riv. It. Palaeont. Strat.*, 117, 221–268. doi: 10.13130/2039-4942/5973
- VENTURINI, C. (1990): Geologia delle Alpi Carniche Centro Orientali.– *Comune di Udine, Museo Friulano di Storia Naturale, Udine*.
- VENTURINI, C. (2006): Evoluzione geologica delle Alpi Carniche.– *Ed. mus. Friulano stor. Nat.*, 48, 1–208.
- WRIGHT, V.P. (1992): A revised classification of limestones.– *Sed. Geology*, 76, 177–185. doi: 10.1016/0037-0738(92)90082-3
- ZANINETTI, L., RETTORI, R. & MARTINI, R. (1994): *Aulotortus ? eotriasicus*, n.sp., un nuovo foraminifero del Trias medio (Anisico) delle Dinaridi ed Ellenidi.– *Boll. Soc. Palaeont. Ital.*, 33, 43–49.